Bone 60 (2014) 162–171

Contents lists available at ScienceDirect

Bone

journal homepage: www.elsevier.com/locate/bone

Original Full Length Article

A myostatin and activin decoy receptor enhances bone formation in mice

P. Bialek *, J. Parkington [1], X. Li [2], D. Gavin, C. Wallace, J. Zhang [1], A. Root, G. Yan, L. Warner [3], H.J. Seeherman [4], P.J. Yaworsky

Biotherapeutics Research and Development, Pfizer Inc., 200 CambridgePark Drive, Cambridge, MA 02140, USA

ARTICLE INFO

Article history:
Received 7 June 2013
Revised 25 November 2013
Accepted 3 December 2013
Available online 9 December 2013

Edited by: Rene Rizzoli

Keywords:
Myostatin
Bone histomorphometry
ActRIIB-Fc
Mechanical testing
Rodent
BMP3

ABSTRACT

Myostatin is a member of the bone morphogenetic protein/transforming growth factor-β (BMP/TGFβ) superfamily of secreted differentiation factors. Myostatin is a negative regulator of muscle mass as shown by increased muscle mass in myostatin deficient mice. Interestingly, these mice also exhibit increased bone mass suggesting that myostatin may also play a role in regulating bone mass. To investigate the role of myostatin in bone, young adult mice were administered with either a myostatin neutralizing antibody (Mstn-mAb), a soluble myostatin decoy receptor (ActRIIB-Fc) or vehicle. While both myostatin inhibitors increased muscle mass, only ActRIIB-Fc increased bone mass. Bone volume fraction (BV/TV), as determined by microCT, was increased by 132% and 27% in the distal femur and lumbar vertebrae, respectively. Histological evaluation demonstrated that increased BV/TV in both locations was attributed to increased trabecular thickness, trabecular number and bone formation rate. Increased BV/TV resulted in enhanced vertebral maximum compressive force compared to untreated animals. The fact that ActRIIB-Fc, but not Mstn-mAb, increased bone volume suggested that this soluble decoy receptor may be binding a ligand other than myostatin, that plays a role in regulating bone mass. This was confirmed by the significant increase in BV/TV in myostatin deficient mice treated with ActRIIB-Fc. Of the other known ActRIIB-Fc ligands, BMP3 has been identified as a negative regulator of bone mass. However, BMP3 deficient mice treated with ActRIIB-Fc showed similar increases in BV/TV as wild type (WT) littermates treated with ActRIIB-Fc. This result suggests that BMP3 neutralization is not the mechanism responsible for increased bone mass. The results of this study demonstrate that ActRIIB-Fc increases both muscle and bone mass in mice. Therefore, a therapeutic that has this dual activity represents a potential approach for the treatment of frailty.

Introduction

Myostatin/growth and differentiation factor 8 (Mstn/GDF8) is a member of the bone morphogenetic protein/transforming growth factor-β (BMP/TGFβ) superfamily of secreted differentiation factors. Myostatin null mice (*Mstn*−/−) develop muscles that are 100–200% larger than littermate controls due to a combination of muscle fiber hyperplasia and hypertrophy [1]. Consistent with its role in mice, genetic loss of myostatin has been associated with increased muscle mass in many different species including sheep [2], cattle [3–5], zebrafish [6,7], dogs [7,8] and humans [9]. Importantly, dogs with only a single functional myostatin allele have improved muscle function [9]. Pharmacological inhibition of myostatin activity in rodents by administration of either neutralizing myostatin antibodies, mutant myostatin propeptides or decoy myostatin receptor-fusion proteins results in increased muscle mass and improved muscle function in both normal and dystrophic animals [11]. In addition, a soluble decoy receptor administered in a single ascending dose study in humans resulted in increased muscle mass as measured by MRI [12]. Collectively, the data imply that inhibiting myostatin activity in humans may result in increased muscle mass and function in a variety of muscle disorders including muscular dystrophy, cancer cachexia, disuse atrophy and sarcopenia.

The biological function of myostatin in skeletal muscle is well studied and new roles for myostatin in other physiological systems are beginning to emerge. Myostatin has been viewed as a myokine [13,14] and its expression has been detected in white fat, cardiomyocytes and bone, suggesting that myostatin may regulate homeostasis in all of these tissues [15,16]. Myostatin was shown to inhibit adipogenesis in primary pre-adipocyte bovine cultures and has been implicated in adipocyte

* Corresponding author.
E-mail address: peter.bialek@pfizer.com (P. Bialek).
[1] Present address: Novartis Institutes for BioMedical Research, Cambridge, MA, USA.
[2] Present address: Perkin Elmer, Waltham, MA, USA.
[3] Present address: Sarepta Therapeutics, Boston, MA, USA.
[4] Present address: Bioventus, Boston, MA, USA.

8756-3282
http://dx.doi.org/10.1016/j.bone.2013.12.002

proliferation [17]. This has further ramifications since adipocytes expresses adipokines such as leptin which regulate food intake, energy expenditure and bone mass through the CNS [18]. Myostatin expression is elevated following cardiomyocyte damage and it has been directly linked to cachexic loss of muscle mass in heart failure patients [19]. A role for myostatin in bone homeostasis has been investigated as well. Examination of bones from myostatin null mice has revealed improved bone strength and bone mineral density in the limbs [20–22], L5 vertebrae [23] and jaw [24]. It is unclear from these studies if the increased bone mass is due to adaptive responses caused by increased load from larger muscles at these attachment sites rather than a direct effect of myostatin signaling in bone or simply due to developmental related effects. More recently, it has been shown that myostatin is expressed at the fracture callus following injury [25]. In addition, myostatin null mice have increased blastema size, total osseous tissue and callus strength in a fibular osteotomy model [26]. The authors suggest that myostatin may regulate the initial recruitment and proliferation of progenitor cells in the callus. Together these data support a role for myostatin in bone homeostasis and repair.

Similar to other members of the BMP family, myostatin activates signaling upon binding to a heterodimeric complex made up of two type 2 receptors: Activin Receptor 2B/2A (ActRIIB)/ActRIIA and two type 1 receptors: Activin Receptor-Like Kinase 4/5 (Alk4/Alk5) [27]. Signals are transduced via Smad2/3 phosphorylation followed by translocation into the nucleus to modulate transcription. Both activin receptors, ActRIIA and ActRIIB, can bind multiple ligands [28,29] including myostatin although with different affinities [30]. Intact and ovariectomized mice treated with a soluble ActRIIA receptor have been reported to have induced bone formation, bone volume and biomechanical strength [31]. Interestingly, these treated animals had no reported increase in body weight or muscle mass. While a soluble ActRIIA molecule has been shown to neutralize myostatin activity in an in vitro model of cell differentiation, the lack of any reported muscle phenotype in vivo may be due to differences in ligand binding affinities or pharmacokinetic properties of the protein [28]. In contrast, mice treated with a soluble ActRIIB receptor demonstrate a dramatic increase in body weight and isolated muscle mass [32]. Furthermore, it was shown that the soluble ActRIIB receptor increased muscle mass in the myostatin null mice suggesting that additional ActRIIB ligands may function as negative regulators of skeletal muscle. ActRIIB is known to be expressed on the surface of many cell types including osteoblasts [33] and research has shown bone marrow stromal cells (BMSCs) isolated from the myostatin null mice express ActRIIB and have enhanced osteogenic potential [34]. Collectively, these data support a potential role of myostatin as well as other ActRIIB ligands in regulating bone homeostasis.

Of all the TGFβ family members, BMP3 and activins (ligands of ActRIIB) are highly expressed in bone [35]. While data supports a role for activins as both positive and negative regulators of bone, the role of BMP3 as a negative regulator of bone is better documented. Osteoblasts and osteocytes secrete BMP3 and targeted deletion of BMP3 results in increased bone mass [36,37]. Further analyses revealed that BMSCs isolated from BMP3 null mice showed an increase in colony number, size and ability to differentiate into osteoblasts [36]. Interestingly, transgenic overexpression of BMP3 in mice leads to delayed osteogenesis and spontaneous rib fractures [38]. Additional in vitro experiments demonstrated that BMP3 can antagonize both BMP2 and BMP4 through an ActRIIB dependent mechanism [36]. The data strongly supports BMP3 as a negative regulator of bone health.

This study evaluated the role of myostatin in regulating bone mass in young adult mice using two distinct pharmacologic inhibitors, a neutralizing antibody to myostatin and a soluble myostatin decoy receptor (ActRIIB-Fc). In addition, studies were performed in both *Mstn*−/− and *Bmp3*−/− mice to begin to define the therapeutic mechanism of action of ActRIIB-Fc. The results of these studies indicate that ActRIIB-Fc modulates bone mass primarily through myostatin and BMP3-independent mechanisms.

Materials and methods

Animals and study design

Female C57BLJ/6 mice were purchased from Charles River Laboratory and group housed (Charles River Laboratory, Andover MA). Myostatin (Mstn) and BMP3 knockout colonies were housed and managed by Taconic (Taconic, Germantown NY, USA). All animals were maintained in a facility with a 12 h light–dark cycle and fed standard mouse pelleted food (PMI Feeds Chow #5001 PharmaServ, Framingham, MA) and water ad libitum. All animal procedures were approved by the Institutional Animal Care and Use Committee (IACUC) and were carried out under the Association for Assessment and Accreditation of Laboratory Animal guidelines.

8 week old female C57BLJ/6, *Mstn*−/− or *Bmp3*−/− mice were administered either weekly intraperitoneal injections (i.p.) of vehicle (Veh) (PBS or Tris–sucrose, n = 8), a neutralizing antibody to myostatin (60 mg/kg JA16, Pfizer, Cambridge MA, n = 8) or a soluble myostatin decoy receptor (10 mg/kg ActRIIB-Fc, Pfizer, Cambridge, MA, n = 8) for a period of 4 weeks. The neutralizing antibody has previously been shown to inhibit GDF-8 and -11 but not other members of the TGFβ family such as activin A, while the decoy receptor was shown to inhibit many members of the TGFβ family including GDF-8, -11 and activins A, B and AB [28,39]. Comparing the effects of both molecules on muscle and bone mass allowed the authors to determine the specific contribution of myostatin inhibition to these studies. The doses were chosen based on previous experiments with these molecules and reflect optimal doses to observe increased muscle mass. The construction, expression and purification of ActRIIB-Fc were previously described [32]. The mouse Mstn monoclonal antibodies (clone JA16) were generated and purified as previously described [40]. In studies involving *Mstn*−/− and *Bmp3*−/− mice, age-matched wild type (WT) littermates were used as controls. Daily subcutaneous injections of 100 μg/kg parathyroid hormone (PTH) (Calbiochem, EMD Chemicals Inc., Gibbston NY, USA), a known bone anabolic agent, were administered to WT mice for 4 weeks to compare the effects with the two myostatin inhibitors.

Body weight was monitored weekly and the dosages/kg were adjusted for changes in body weight. In all of the above studies, fluorochrome bone labels were administered to all animals 10 and 2 days before the end of the study to quantify bone formation. After 4 weeks of treatment, mice were euthanized by CO_2 asphyxiation and blood was collected by cardiac puncture. Serum samples were initially stored for 30 min at 4 °C, then centrifuged for 10 min at 10 K rpm and stored at −20 °C. Gastrocnemius and quadricep muscles were isolated from both limbs and the weights recorded. The L4 and L5 lumbar vertebrae and both left and right femora were also harvested. The residual muscle, ligament and tendon tissues were removed. The L5 vertebrae and left femora were stored in 70% ethanol and were used for histological evaluation. The L4 vertebrae and right femora were wrapped in PBS soaked-gauze, frozen at −20 °C and were used for biomechanical testing.

Micro-computed tomography (μCT) analysis

L5 vertebrae and distal femora were imaged using a Scanco MCT40 (Scanco Medical AG, Brassersdorg, Switzerland) at a 12 μm isotropic voxel size. Transverse slices were acquired for the entire length of the L5 vertebral body. Vertebral trabecular bone was assessed in the region immediately distal to the cranial growth plate and immediately proximal to the caudal growth plate resulting in an evaluated region of ~2000 μm. Transverse slices were obtained starting at the midpoint of the distal growth plate and extending proximally for 3000 μm. For the distal femora, trabecular bone was assessed over a 1500 μm region immediately proximal to the distal growth plate. Trabecular bone for both the L5 vertebrae and distal femur was defined by automated contouring to the endosteal surface using an inner value of 8 and outer value of 388. Automated contours were defined every 120 mm and remaining

contours were created using an adaptive–iterative algorithm [41]. Bone volume fraction (BV/TV), trabecular thickness (Tb.Th) and trabecular number (Tb.N) were calculated based on automated analyses. For cortical thickness analyses, a 120 μm region of the distal femur was evaluated 2500 μm proximal to the growth plate.

Histological evaluation

The L5 vertebral bodies and left femur were cut transversely along the midline with a band saw equipped with a diamond blade. The specimens were fixed in 70% ethanol, dehydrated in graded concentrations of ethanol, defatted in acetone, and embedded without decalcification in methyl methacrylate. 8.0 μm and 10.0 μm sagittal sections were cut using a microtome (Reichert Junt Polycut S, Cambridge Instruments, Heidelberg, Germany) for histomorphometric measurements as described previously [42]. The 8-μm sections were stained with modified Von Kossa stain while the 10-μm section remained unstained. Static and dynamic histomorphometric measurements of lumbar vertebral trabecular bone were calculated using a computerized digital microscopy histomorphometry analysis system (OsteoMeasure, OsteoMetrics, Inc., Decatur, GA, USA). Total tissue area, trabecular bone area, and trabecular bone perimeter were measured from the 8.0 μm thick sections. Trabecular bone volume, trabecular number, trabecular thickness, and trabecular separation were calculated as described previously [42]. Single-calcein labeled perimeter, double-calcein labeled perimeter, and interlabel width were measured on the 10 μm sections. These data were used to calculate percent labeled trabecular surface, mineral apposition rate and bone formation rate-surface as described previously [42].

Evaluation of serum markers

Serum calcium was determined using the Quantichrom Calcium assay (Bioassay Systems, Hayward, CA). Serum osteocalcin was determined using the Osteocalcin ELISA (Biomedical Technologies Inc., Stoughton, MA). C-telopeptide fragments of collagen Type I (CTX-1) in serum was determined using the RATLAPS ELISA kit (Nordic Bioscience, Herlev, Denmark). Serum procollagen type I N-propeptide (P1NP) was determined using the PINP ELISA (Immunodiagnostic Systems Ltd., Fountain Hills, AZ). All assays were performed following the manufacturer's protocols.

Biomechanical testing

Prior to testing, L4 vertebrae were thawed at room temperature and both growth plates were removed. Vertebral bodies were tested in compression using a materials testing machine (Model 5565, Instron, Norwood, MA) and a 100 N load cell. Load was applied at a constant rate of 3 mm/min until failure. Maximum load and stiffness were collected from force–displacement curves using Bluehill software version 2.14 (Instron, Norwood, MA). The right femora were potted in hex nuts using methyl methacrylate and tested in torsion using a material testing machine (Model 55MT, Instron, Norwood, MA) and a 2 Nm load cell. The femora were internally rotated and were tested at a constant rate of 1°/s until failure. Maximum torque and energy to failure were calculated using Partner software version 6.3a (Instron Satec, Norwood, MA).

Statistical analysis

Results are expressed as the mean ± standard deviation. Comparisons between two groups were performed using the unpaired Student *t*-test or the Wilcoxon–Mann–Whitney exact test. Mouse strain, treatment and their interaction were included in the ANOVA model. The interaction term was used to investigate if there was a differential effect of treatment due to the genetic differences in the mice. All tests were considered significant when $p < 0.05$.

Results

ActRIIB-Fc is an anabolic bone agent

We have previously demonstrated that ActRIIB-Fc is a potent myostatin inhibitor that can increase muscle mass in normal and dystrophic animals [10]. To study the effects of ActRIIB-Fc on bone, mice were administered ActRIIB-Fc for 4 weeks. Young adult female mice were used to allow us to compare our results to our previous data. PTH was included as a comparator as a known anabolic agent. Mice treated for 4 weeks with ActRIIB-Fc increased body weight by 18% compared to vehicle treated control mice (Table 1). Gastrocnemius and quadriceps muscle masses were increased by 16.4% and 19.1% respectively compared to vehicle-treated controls (Table 1). These data are consistent with previous results confirming ActRIIB-Fc as an anabolic muscle agent. Mice treated for 4 weeks with PTH did not show a difference in body weight compared to vehicle-treated controls. Interestingly, quadricep but not gastrocnemius muscle mass was significantly decreased by 9% in the PTH-treated mice compared to vehicle-treated mice at 4 weeks. MicroCT (μCT) analyses demonstrated that mice treated for 4 weeks with ActRIIB-Fc had a significant increase in BV/TV in the distal femora (132%) and L5 vertebrae (27%) compared to vehicle-treated controls (Fig. 1A). The increase in BV/TV in the distal femora of ActRIIB-Fc treated mice was due to an increase in both trabecular thickness and trabecular number (Figs. 1B and C). Only trabecular thickness was significantly increased in the vertebrae. Cortical thickness and density was unchanged in the femora of ActRIIB-Fc-treated mice while treatment with PTH increased femoral cortical thickness and density (Fig. 1D). MicroCT analyses demonstrated that mice treated for 4 weeks with PTH had a significant increase in BV/TV in the distal femora (61%) but not in the L5 vertebrae (10%) compared to vehicle-treated controls (Fig. 1A and D). Fig. 2 shows representative μCT images of trabecular bone from distal femurs from mice treated with either vehicle, ActRIIB-Fc or PTH.

To understand better the dramatic increased trabecular bone BV/TV in the ActRIIB-Fc-treated mice, static and dynamic histomorphometry was performed on the femur and L5 vertebrae. Static histomorphometry evaluation confirmed the μCT data and showed that both ActRIIB-Fc and PTH increased bone mass (Supplemental Table 1). Calcein double-labeling demonstrated that the bone formation rate (BFR) was increased in the femurs and L5 vertebrae by 249% and 174% respectively in ActRIIB-Fc treated mice compared to vehicle-treated animals (Table 2). Increased bone formation rate was associated with increased mineralization surface (MS) and mineralization apposition rate (MAR) at both sites (Table 2). As expected, PTH treatment increased bone formation rate 112% in femurs and 69% in L5 vertebrae compared to vehicle-treated animals. Increased BFR in the femur was associated with increased MS and MAR while only MAR was significantly increased in the vertebrae. Therefore both ActRIIB-Fc and PTH increased bone mass by enhancing the bone formation rate.

To confirm the anabolic effect of ActRIIB-Fc and PTH, we analyzed serum markers of osteoblast and osteoclast activity. Serum calcium levels were significantly increased in ActRIIB-Fc treated mice (7%)

Table 1
Effect of ActRIIB-Fc on body weight and muscle mass.

Parameters	Vehicle	ActRIIB-Fc	PTH
Body weight			
Wk 0 (grams)	22.5 ± 1.3	21.9 ± 1.0	22.3 ± 1.2
Wk 4 (grams)	22.5 ± 1.2	23.8 ± 1.6	22.7 ± 1.4
Muscle weights			
Gastroc (mg)	136.9 ± 8.1	160.1 ± 10.0[a]	127.3 ± 5.9
Quadriceps (mg)	180.3 ± 11.3	214.8 ± 18.9[a]	163.7 ± 4.8[a]

Data shown are means ± SD.
[a] $p < 0.05$ vs. vehicle.

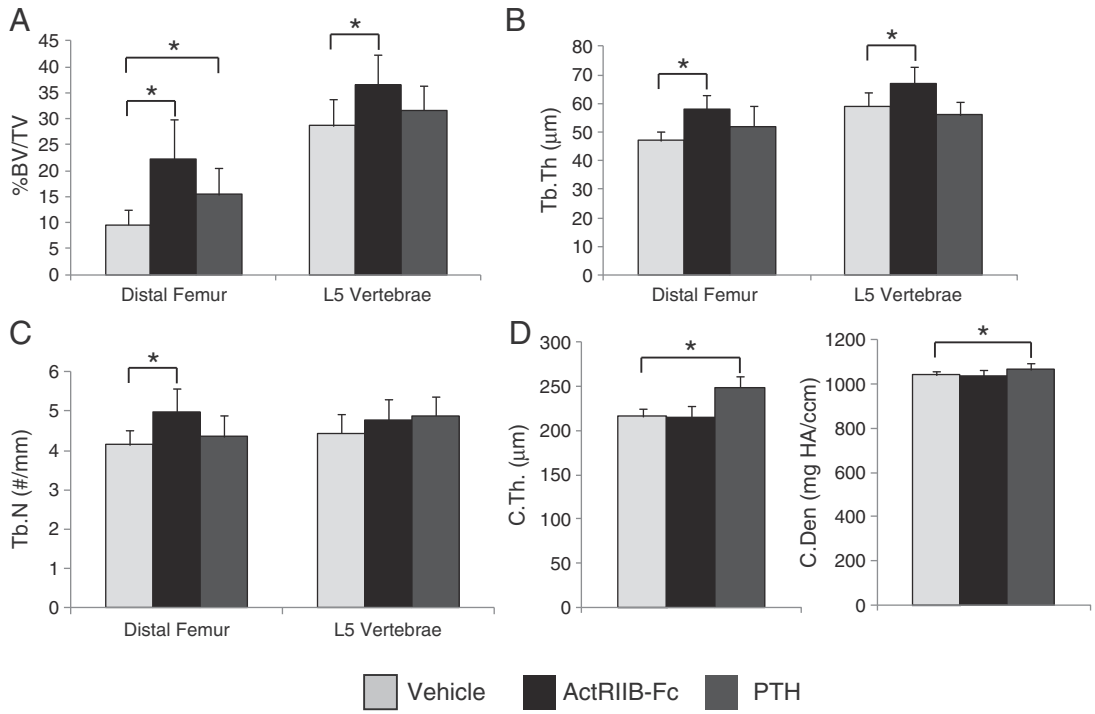

Fig. 1. ActRIIB-Fc effects trabecular but not cortical bone. μCT analyses of mice treated for 4 weeks with either vehicle, ActRIIB-Fc or PTH. (A) Trabecular bone volume fractions BV/TV (%), (B) trabecular thickness Tb.Th (μm) and (C) trabecular number Tb.N (#/mm) were measured in the distal femora and L5 vertebrae. (D) Cortical thickness C.Th (μm) and density C.Den (mg HA/cm^3) were measured in the femur mid-shaft. Results are presented as mean ± SD (n = 7–10 per group). Statistical differences from controls are indicated by*p < 0.05.

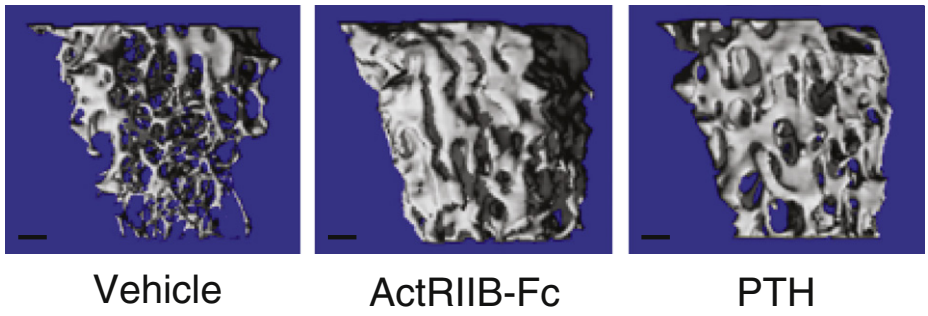

Fig. 2. ActRIIB-Fc and PTH increase trabecular bone volume in the femur. Representative images of reconstituted μCT data. Bar represents 300 μm.

compared to vehicle-treated animals (Table 3). Curiously, significant changes were not observed in bone serum anabolic markers such as of osteocalcin or P1NP. Similarly, no changes were detected in CTx, a serum biomarker of bone resorption, following treatment with ActRIIB-Fc. In contrast, mice treated with PTH, a known activator of osteoblast activity, showed significantly increased serum calcium (9%), osteocalcin (25%) and P1NP (82%) (Table 3). Serum CTx levels remained unchanged in PTH treated mice.

To differentiate the effects of ActRIIB-Fc and PTH on bone quality, vertebral compression and femora torsional strength were assessed. Mice treated with ActRIIB-Fc showed a significantly increased maximum compressive failure load (18%) and stiffness (44%) in L4 vertebrae at 4 weeks compared to vehicle-treated animals (Table 4). Maximum torsional load, energy and stiffness of the femora were not increased following treatment with ActRIIB-Fc. Mice treated with PTH did not show significant improvement in maximum compressive load or stiffness in L4 vertebrae compared to vehicle-treated mice. However, torsional

Table 2
Effect of ActRIIB-Fc on dynamic histomorphometry parameters.

Parameter	Vehicle	ActRIIB-Fc	PTH
Distal femora			
MS (%)	15.92 ± 3.61	39.68 ± 5.94[a,b]	29.28 ± 6.47[a]
MAR (μm/d)	1.01 ± 0.15	1.42 ± 0.17[a,b]	1.18 ± 0.1[a]
BFR (m^3/mm^2/yr)	0.059 ± 0.019	0.206 ± 0.043[a,b]	0.125 ± 0.027[a]
L5 vertebrae			
MS (%)	12.37 ± 4.4	24.43 ± 6.3[a,b]	17.69 ± 6.22
MAR (μm/d)	0.89 ± 0.12	1.19 ± 0.14[a,b]	0.99 ± 0.03[a]
BFR (m^3/mm^2/yr)	0.039 ± 0.01	0.107 ± 0.035[a,b]	0.064 ± 0.023[a]

Data shown are means ± SD.
[a] p < 0.05 vs. vehicle.
[b] p < 0.05 vs. PTH.

Table 3
Effect of ActRIIB-Fc on serum biochemistry.

Parameters	Vehicle	ActRIIB-Fc	PTH
Calcium (ng/ml)	10.0 ± 0.5	10.7 ± 0.4[a]	10.9 ± 0.5[a]
Osteocalcin (ng/ml)	88.4 ± 16.6	81.4 ± 20.8	110.3 ± 22.1[a]
P1NP (ng/ml)	6.3 ± 0.5	6.7 ± 1.7	11.5 ± 4.0[a]
CTX-1 (ng/ml)	25.4 ± 4.5	39.5 ± 25.9	27.0 ± 8.3

Data shown are means ± SD.
[a] p < 0.05 vs. vehicle.

Table 4
Effect of ActRIIB-Fc on bone structural analyses.

Parameters	Vehicle	ActRIIB-Fc	PTH
L4 vertebrae			
Failure to load (N)	34 ± 3.1	40 ± 5.9[a]	32 ± 7.4
Stiffness (N/mm)	95 ± 45.8	137 ± 24.2[a]	109 ± 29.9
Femora			
Max torsional (N·mm)	21.0 ± 8.1	22 ± 4.7	29 ± 4.5[a]
Energy (mJ)	1.9 ± 1.0	2.0 ± 1.2	3.0 ± 1.0[a]
Stiffness (N·mm/rad)	156.3 ± 40.0	161.3 ± 53.0	186.6 ± 35.7

Data shown are means ± SD.
[a] $p < 0.05$ vs. vehicle.

Table 5
Effect of Mstn-mAb on body weight and muscle mass.

Parameters	Vehicle	Mstn-mAb
Body weight		
Wk 0 (grams)	17.6 ± 0.8	17.8 ± 0.7
Wk 4 (grams)	18.3 ± 1.1	20.5 ± 1.2
Muscle weights		
Gastroc (mg)	116.7 ± 8.5	139.8 ± 13.8[a]
Quadriceps (mg)	148.6 ± 11.1	178.3 ± 14.6[a]

Data shown are means ± SD.
[a] $p < 0.05$ vs. vehicle.

strength was increased in the femora (38%) of PTH-treated animals compared to vehicle-treated femora (Table 4). Together, these data support that bone quality was increased in mice treated with ActRIIB-Fc.

Myostatin mAb increases muscle mass but has no effect on bone

Mice were treated for 4 weeks with a Mstn-mAb to determine if myostatin inhibition alone could explain the increase in both muscle and bone mass observed in ActRIIB-Fc treated mice. At the end of the study, body weight was increased by 15% while gastrocnemius and quadriceps muscle masses were increased by 19.8% and 20% respectively compared to vehicle-treated control mice (Table 5). The increased body weight and muscle mass confirmed anabolic activity in muscle between Mstn-mAb and ActRIIB-Fc. Subsequent μCT analyses did not show significant differences in BV/TV, trabecular thickness or trabecular number in either the distal femora or the L5 vertebrae compared to vehicle treated controls (Fig. 3A–C). In addition, cortical thickness and density remained unchanged in the Mstn-mAb treated mice (Fig. 3D). Histological analyses, biomechanics and serum markers of bone remained unchanged (Supplemental Tables 2–4). Therefore, the data demonstrated that neutralization of myostatin significantly increased muscle mass but had no effects on bone mass.

The anabolic effect of ActRIIB-Fc on bone is predominantly myostatin-independent

The lack of a bone phenotype in Mstn-mAb treated mice was unexpected. To help explain this discrepancy, we analyzed *Mstn*−/− mice from our own colony. As previously described, *Mstn*−/− mice weighed more (25%) and contained larger gastrocnemius and quadriceps muscles (muscle mass was increased 81% and 90% respectively) compared to wild type littermates (Table 6) [1]. μCT analyses of the distal femora but not the L5 vertebrae from *Mstn*−/− mice showed a significant increase in trabecular BV/TV (56%) compared to age-matched wild type littermates (Fig. 4A). The increase in BV/TV was due to increased trabecular number and thickness (Fig. 4B, C). Since the genetic data supported a role for myostatin in bone growth, *Mstn*−/− mice were administered ActRIIB-Fc for 4 weeks. ActRIIB-Fc treatment increased body weight and muscle mass in *Mstn*−/− mice as previously reported [32] (Table 6). *Mstn*−/− mice treated with ActRIIB-Fc showed a further significant increase in BV/TV in distal femora (72%) and L5 vertebrae (39%) relative to age and gender matched *Mstn*−/− mice treated with vehicle (Fig. 4A). The increase in BV/TV was due primarily to an increase in trabecular

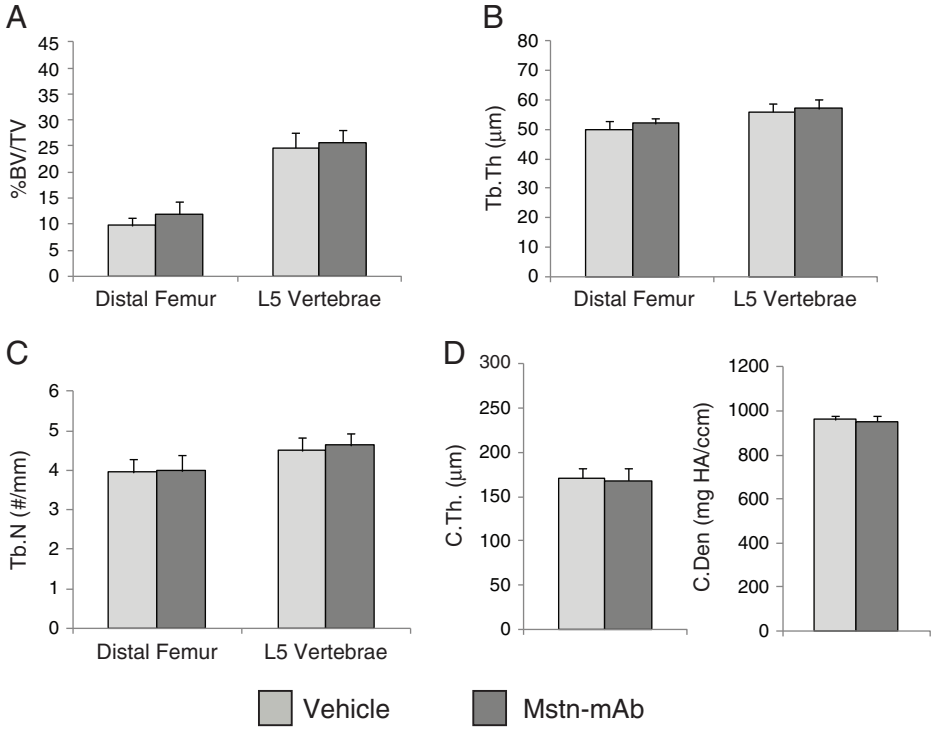

Fig. 3. Mstn-mAb has no effect on bone mass. μCT analyses of mice treated for 4 weeks with either vehicle or a neutralizing myostatin antibody (Mstn-mAb). (A) Trabecular bone volume fractions BV/TV (%), (B) trabecular thickness Tb.Th (μm) and (C) trabecular number Tb.N (#/mm) were measured in the distal femora and L5 vertebrae. (D) Cortical thickness C.Th (μm) and density C.Den (mg HA/cm^3) were measured in the femur mid-shaft. Results are presented as mean ± SD (n = 7–10 per group). Statistical differences from controls are indicated by*$p < 0.05$.

Table 6
Effect of ActRIIB-Fc on body weight and muscle mass in *Mstn*−/− and WT littermates.

	Wild type		*Mstn*−/−	
Parameter	Vehicle	ActRIIB-Fc	Vehicle	ActRIIB-Fc
Body weight				
Wk 0 (grams)	20.1 ± 1.9	18.9 ± 1.1	25.0 ± 0.9[b]	23.3 ± 0.3
Wk 4 (grams)	21.0 ± 1.9	24.7 ± 2.0[a]	26.2 ± 1.0	29.5 ± 1.0[a]
Muscle weights				
Gastroc (mg)	129.5 ± 9.1	166.0 ± 4.0[a]	234.4 ± 24.7[b]	278.3 ± 24.3[a]
Quadriceps (mg)	170.3 ± 11.9	224.5 ± 10.1[a]	323.2 ± 29.6[b]	371.9 ± 25.9[a]

Data shown are means ± SD.
[a] $p < 0.05$ vs. vehicle.
[b] $p < 0.05$ vs. WT littermates.

thickness and trabecular number in both bones (Fig. 4B, C). As a control, WT littermates were also treated for 4 weeks with ActRIIB-Fc. Body weight, muscle mass and bone mass were increased similar to data presented above (compare Tables 1 and 6 and Figs. 1 and 4). ANOVA analyses determined that ActRIIB-Fc had a similar effect on bone parameters on *Mstn*−/− and their WT littermates. Taken together, these pharmacologic and genetic data suggest that the anabolic bone effect of ActRIIB-Fc involves inhibition of additional ligands other than myostatin.

The anabolic effect of ActRIIB-Fc on bone is BMP3 independent

One potential bone related ligand that signals through the ActRIIB receptor is BMP3 [37]. To investigate if the anabolic bone activity of

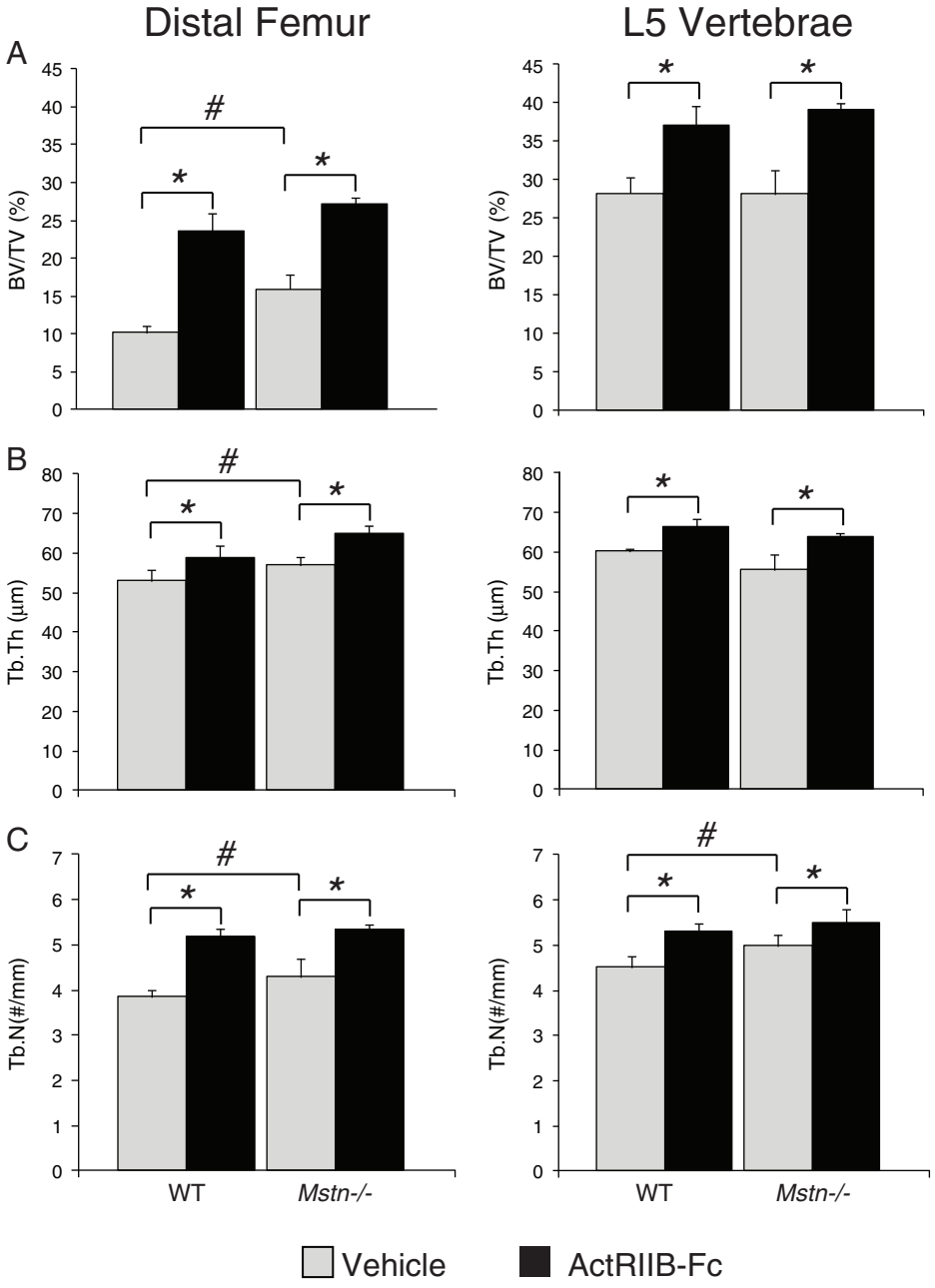

Fig. 4. ActRIIB-Fc increases trabecular bone volume in *Mstn*−/− mice. μCT analysis of distal femora and L5 vertebrae from *Mstn*−/− or wild type (WT) littermates treated with either vehicle or ActRIIB-Fc for 4 weeks. Shaded bars represent vehicle-treated mice and solid bars represent ActRIIB-Fc-treated mice. (A) Trabecular bone volume fractions Tb BV/TV (%), (B) Trabecular thickness Tb.Th (μm) and (C) Trabecular number Tb.N (#/mm) were measured in the distal femora and L5 vertebrae. Results are presented as mean ± SD (n = 5–6 per group). Statistical differences from controls due to treatment are indicated by *$p < 0.05$. Statistical differences due to genotype are indicated by #$p < 0.05$.

Table 7
Effect of ActRIIB-Fc on body weight and muscle mass in *Bmp3*−/− and WT littermates.

	Wild type		*Bmp3*−/−	
Parameter	Vehicle	ActRIIB-Fc	Vehicle	ActRIIB-Fc
Body weight				
Wk 0 (grams)	22.5 ± 1.3	21.9 ± 1.0	19.7 ± 2.3[b]	20.7 ± 1.6
Wk 4 (grams)	22.5 ± 1.2	23.8 ± 1.6	21.0 ± 3.1	22.8 ± 2.5
Muscle weights				
Gastroc (mg)	136.9 ± 8.1	160.1 ± 10.0[a]	122.4 ± 15.9[b]	156.7 ± 11.6[a]
Quadriceps (mg)	180.3 ± 11.3	214.8 ± 18.9[a]	162.9 ± 16.8[b]	210.6 ± 19.1[a]

Data shown are means ± SD.
[a] $p < 0.05$ vs. vehicle.
[b] $p < 0.05$ vs. WT littermates.

ActRIIB-Fc is due to BMP3 neutralization, *Bmp3*−/− mice were analyzed. *Bmp3*−/− mice were smaller than the wild type littermates at the start of the study (Table 7). As expected, μCT analyses of untreated *Bmp3*−/− mice demonstrated increased BV/TV of distal femur (60%) and L5 vertebrae (16%) compared to age-matched WT littermates (Fig. 5A). The elevated BV/TV bone mass was due to increased trabecular thickness and trabecular number in the distal femora and increased trabecular number in the vertebrae (Figs. 5B, C). Following 4 weeks of ActRIIB-Fc treatment, *Bmp3*−/− mice gained 8.6% body mass and increased gastrocnemius and quadricep muscle mass was by 28% and 29.3% respectively compared to vehicle treated *Bmp3*−/− mice (Table 7). *Bmp3*−/− animals treated with ActRIIB-Fc showed significantly increased BV/TV in the distal femora (93%) and L5 vertebrae (57%) compared to vehicle-treated *Bmp3*−/− mice (Fig. 5A). The increase in BV/TV in both femur and vertebrae was due to an increase in trabecular thickness and trabecular number. WT littermates treated for 4 weeks with ActRIIB-Fc also showed similar increases in BV/TV in the distal femora and L5 vertebrae (131% and 30% respectively). ANOVA analyses determined that ActRIIB-Fc treatment had a similar effect on bone parameters on *Bmp3*−/− and their WT littermates. These results indicate that the anabolic effect of ActRIIB-Fc on bone does not involve neutralization of BMP3 activity.

Discussion

The role of myostatin in regulating muscle mass has been extensively studied in normal and pathological conditions but a putative role in regulating bone mass has not been as thoroughly investigated [11]. The analyses of *Mstn*−/− mice identified increased trabecular bone in the distal femora but not the vertebrae in 12 week old females. In 12 week-old male *Mstn*−/− mice, increased trabecular bone was also observed in the vertebrae but not in the distal femora (data not shown). In addition, cortical bone was unchanged. Differences in bone parameters observed in this study compared to published reports may be explained by differences in age, sex, methods of analyses and colony-specific effects [20,22]. The aggregate of the genetic data does support a role for myostatin in regulating bone mass, albeit, a potentially developmental one. *Mstn*−/− mice treated with ActRIIB-Fc showed an anabolic activity in both muscle and bone at all sites analyzed suggesting that myostatin is only one of the several ligands antagonized by ActRIIB-Fc that are important in homeostasis.

Mice treated with either Mstn-mAb or ActRIIB-Fc showed modest increases in muscle mass in this study but only treatment with ActRIIB-Fc resulted in a dramatic increase in BV/TV in L5 vertebrae and distal femora. Interestingly, the distal femora from mice treated with the Mstn-mAb showed a trend towards increased BV/TV. It is possible that prolonged administration of Mstn-mAb beyond 4 weeks may result in increased bone mass and strength. The lack of a significant improvement to bone by a Mstn-mAb also suggests that the adaptation of bone to increased muscle mass is a slower process than expected. On the other hand, unloading of bone by reduction of gravity during space flight or hindlimb suspension in rodents results in a rapid loss of bone mass [43–46]. Recently, data demonstrated that bone mass can be increased via in vivo mechanical loading of the tibia [47]. Our data demonstrates that a rapid gain in muscle mass does not translate to a rapid gain in bone mass, suggesting that the effect of ActRIIB-Fc on bone involved other regulatory pathways.

Both molecules inhibit myostatin activity in cell-based reporter assays and both increase muscle mass in vivo [32,48]. The differential effects of Mstn-mAb and ActRIIB-Fc on bone are likely due to the inhibition of other TGFβ/BMP ligands or other non-TGFβ/BMP ligands by ActRIIB-Fc. Several labs have demonstrated that ActRIIB-Fc can interact with many of these secreted factors in mouse and human serum and modulates their activities [28,49,50]. The role of ligands other than myostatin in the modulation of both muscle and bone mass is likely given the fact that *Mstn*−/− mice treated with ActRIIB-Fc gain additional muscle mass [32] and show increased BV/TV at multiple sites as reported here.

The role of BMP3 as a potential ligand responsible for ActRIIB-Fc's anabolic activity on bone was investigated in this study. Previous reports demonstrated that Bmp3 −/− animals exhibit increased bone mass [37] as we have now independently confirmed here. This is consistent with BMP3's ability to inhibit osteoblast differentiation of bone marrow cells in vitro [36]. Interestingly, BMP3 requires ActRIIB to inhibit osteoblast differentiation even though it can bind to both type II activin receptors, ActRIIA and ActRIIB. This study demonstrated that ActRIIB-Fc increased trabecular bone volume in *Bmp3*−/− mice and their WT littermates to the same extent. If BMP3 inhibition by ActRIIB-Fc was primarily responsible for the increased bone mass, then BV/TV should be similar to WT mice treated with ActRIIB-Fc compared to *Bmp3*−/− controls and that ActRIIB-Fc would not increase BV/TV in the *Bmp3*−/− animals. The observation that ActRIIB-Fc significantly increased bone mass in *Bmp3* null mice to the same extent as WT mice suggests that BMP3 neutralization is not required for the anabolic activity of ActRIIB-Fc on bone. Increased bone mineral density following treatment with ActRIIA-Fc in *Bmp3*−/− mice was previously reported but this is first report to demonstrate this by ActRIIB-Fc [31,51,52].

ActivinA is also highly expressed in bone but the role of activins and their antagonists in bone metabolism both in vitro and in vivo has demonstrated conflicting results [53]. In bone-marrow derived osteoclast cultures, activinA stimulates osteoclastogenesis while its effects on cultured osteoblasts is less clear [54,55]. In vivo, activinA has been shown to promote callus formation when directly applied to the fracture site [56]. Furthermore, activinA administration can increase bone mineral density in vertebrae of aged ovariectomized rats [57]. In contrast, transgenic over expression of inhibin, an antagonist of activinA activity, increased bone formation, bone mass and strength [58]. Administration of a soluble decoy receptor of activinA, ActRIIA-mFc, was reported to increase trabecular bone mass and strength by stimulating osteoblast activity [31]. This phenotype is very similar to ActRIIB-Fc treatment although there are some distinct differences. Both agents increased bone mass to a similar extent by stimulating osteoblast activity as measured by dynamic histomorphometry. However only ActRIIA-mFc increased serum osteocalcin expression. Prolonged treatment of ActRIIA-mFc also resulted in increased cortical bone thickness and enhanced femoral strength which was not observed in our shorter ActRIIB-Fc treatment. The similarities in bone phenotypes between ActRIIB-Fc and ActRIIA-Fc certainly suggest that both molecules may antagonize a common ligand or group of ligands responsible for regulating bone mass. ActRIIB-Fc inhibits activinA, activinB and activinAB in cell-based reporter assays with the similar potency as myostatin [28]. Neutralization of one of the activins may be responsible for the enhanced bone phenotype from either or both decoy-receptors. In contrast, ActRIIB-Fc increased muscle mass while ActRIIA-mFc did not, further supporting the hypothesis that some aspects of the regulation of bone mass and muscle mass are independent.

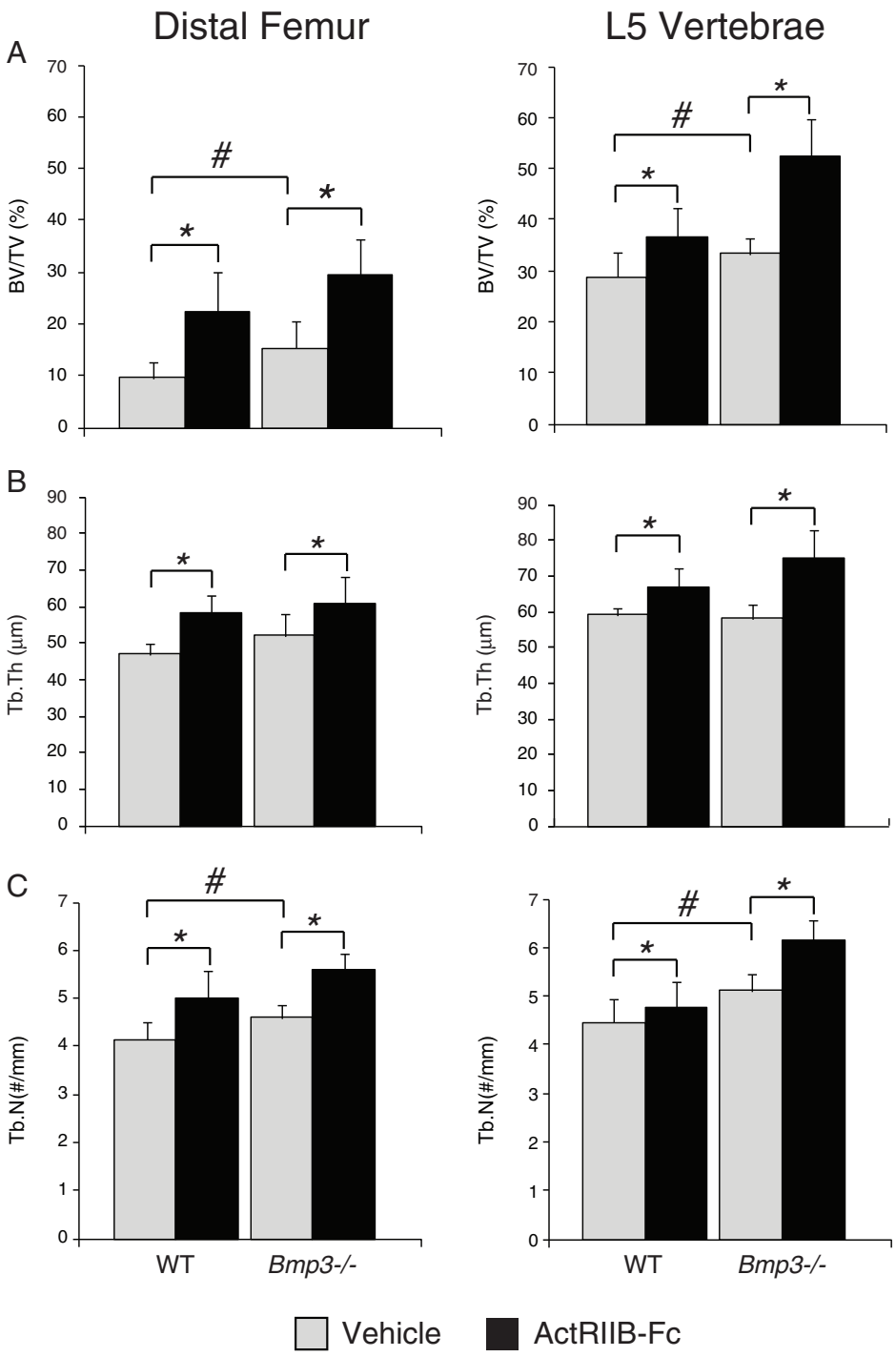

Fig. 5. ActRIIB-Fc increases trabecular bone volume in *Bmp3*−/− mice. μCT analysis of distal femora and L5 vertebrae from *Bmp3*−/− or wild type littermates treated with either vehicle or ActRIIB-Fc. Open bars represent vehicle-treated mice and solid bars represent ActRIIB-Fc-treated mice. (A) Trabecular bone volume fractions Tb BV/TV (%), (B) trabecular thickness Tb.Th (μm) and (C) trabecular number Tb.N (#/mm) were measured in the distal femora and L5 vertebrae. Results are presented as mean ± SD (n = 7–10 per group). Statistical differences from controls due to treatment are indicated by $^{*}p < 0.05$. Statistical differences due to genotype are indicated by $^{\#}p < 0.05$.

The anabolic effect of ActRIIB-Fc on bone was compared to PTH, a known anabolic bone agent [59]. Both therapies increased bone mass and strength but some significant differences in the phenotypes were observed. While PTH increased both trabecular and cortical bone thicknesses in the femur, ActRIIB-Fc dramatically increased femoral trabecular bone but had no effect on cortical bone thickness. This combination of increased trabecular and cortical bone in the femur of PTH treated mice resulted in enhanced torsional strength and stiffness that was not observed in femurs from ActRIIB-Fc treated animals. In contrast, PTH treatment did not significantly increase vertebral bone volume or strength while ActRIIB-Fc increased vertebral trabecular bone volume and enhanced vertebral compression strength. It is tempting to speculate that PTH treatment enhanced periosteal bone formation while ActRIIB-Fc did not. Certainly, dynamic histomorphometry analyses suggest that ActRIIB-Fc and PTH increase trabecular bone formation. Biochemical analyses of serum from PTH treated mice detected increases in sCa, P1NP and osteocalcin which support the evidence that PTH stimulates bone formation. Other than a mild but significant increase in sCa, ActRIIB-Fc treated mice did not display typical changes in either P1NP or osteocalcin which one might expect given the dramatic increase in

trabecular bone formation. It is possible that we missed detecting changes in these anabolic markers by only analyzing serum at the end of the study. Alternatively, it is possible that ActRIIB-Fc and PTH enhance bone formation via different mechanisms. Other groups reported that ActRIIB-Fc treatment increased P1NP in aged mice [60]. In addition, treatment of postmenopausal women with ActRIIB-Fc (ACE-031) demonstrated changes in serum bone turnover markers such as BALP [12]. In both studies, it may be easier to detect changes in these serum markers since osteoblast activity is known to diminish with age in both rodents and humans. It remains unclear why changes in P1NP and osteocalcin were not observed in our study. Additionally, the effect of ActRIIB-Fc on sCa is puzzling. Multiple mechanisms associated with hypercalcemia have been described including elevated PTH, abnormal FGF23 levels, Paget's disease, rheumatoid arthritis, autoimmune responses and cancer. Further studies will be necessary to understand whether ActRIIB-Fc influences sCa directly or if this is through an indirect mechanism.

The dynamic histomorphometry data from this work supports that administration of ActRIIB-Fc for 4 weeks is anabolic to bone. Effects on bone resorption, as measured by serum CTx levels, do not appear to be a major contributor to the measured bone parameters. Similarly, short term intermittent PTH administration, as performed in this study, did not alter CTx levels. In contrast, chronic or sustained PTH signaling and neutralizing antibodies to SOST [61–63] have demonstrated changes in osteoclast activity and in CTx levels in addition to their initial effects on stimulating osteoblast activity. Antiresorptive therapies with diverse mechanism of actions, such as raloxifene, denosumab, strontium ranelate, odanacatib or bisphosphonates demonstrated decreases in CTx or TRAP-5b serum levels [64–68]. Therefore we hypothesize that ActRIIB-Fc would not have a major anti-resorptive contribution to the dramatic increase in trabecular bone without affecting CTx levels.

The results of this study demonstrated that treatment with a neutralizing myostatin antibody increased only muscle mass while treatment with ActRIIB-Fc increased both muscle and bone masses in mice. The anabolic effect of ActRIIB-Fc on muscle mass appears to be the result of inhibition of myostatin and non-myostatin ligands while increased bone mass is largely independent of inhibition of myostatin. More work will be necessary to identify these additional factors that interact with ActRIIB to regulate bone homeostasis. Based on these results, treatment with ActRIIB-Fc may be beneficial not only for diseases associated with muscle atrophy but also for diseases associated with bone loss as well.

Acknowledgments

The authors wish to thank Jane Owens, Julia Billiard, Peter Bodine and Carl Morris for critical review of the manuscript.

Appendix A. Supplementary data

Supplementary data to this article can be found online at http://dx.doi.org/10.1016/j.bone.2013.12.002.

References

[1] McPherron AC, Lawler AM, Lee SJ. Regulation of skeletal muscle mass in mice by a new TGF-beta superfamily member. Nature 1997;387(6628):83–90.
[2] Mateescu RG, Thonney ML. Gene expression in sexually dimorphic muscles in sheep. J Anim Sci 2002;80(7):1879–87.
[3] McPherron AC, Lee SJ. Double muscling in cattle due to mutations in the myostatin gene. Proc Natl Acad Sci U S A 1997;94(23):12457–61.
[4] Smith TP, Lopez-Corrales NL, Kappes SM, Sonstegard TS. Myostatin maps to the interval containing the bovine mh locus. Mamm Genome 1997;8(10):742–4.
[5] Kambadur R, Sharma M, Smith TP, Bass JJ. Mutations in myostatin (GDF8) in double-muscled Belgian Blue and Piedmontese cattle. Genome Res 1997;7(9):910–6.
[6] Xu C, Wu G, Zohar Y, Du SJ. Analysis of myostatin gene structure, expression and function in zebrafish. J Exp Biol 2003;206(Pt 22):4067–79.
[7] Acosta J, Caprio Y, Borroto I, Gonzalez O, Estrada MP. Myostatin gene silenced by RNAi show a zebrafish giant phenotype. J Biotechnol 2005;119(4):324–31.
[8] Shelton GD, Engvall E. Gross muscle hypertrophy in whippet dogs is caused by a mutation in the myostatin gene. Neuromuscul Disord 2007;17(9–10):721–2.
[9] Mosher DS, Quignon P, Bustamante CD, Sutter NB, Mellersh CS, Parker HG, et al. A mutation in the myostatin gene increases muscle mass and enhances racing performance in heterozygote dogs. PLoS Genet 2007;3(5):e79.
[10] Schuelke M, Wagner KR, Stolz LE, Hubner C, Riebel T, Komen W, et al. Myostatin mutation associated with gross muscle hypertrophy in a child. [see comment] N Engl J Med 2004;350(26):2682–8.
[11] Bradley L, Yaworsky PJ, Walsh FS. Myostatin as a therapeutic target for musculoskeletal disease. Cell Mol Life Sci 2008;65(14):2119–24.
[12] Attie KM, Borgstein NG, Yang Y, Condon CH, Wilson DM, Pearsall AE, et al. A single ascending-dose study of muscle regulator ACE-031 in healthy volunteers. Muscle Nerve 2012;47(3):416–23.
[13] Hamrick MW. A role for myokines in muscle–bone interactions. Exerc Sport Sci Rev 2011;39(1):43–7.
[14] Havekes B, Sauerwein HP. Adipocyte–myocyte crosstalk in skeletal muscle insulin resistance; is there a role for thyroid hormone? Curr Opin Clin Nutr Metab Care 2010;13(6):641–6.
[15] Feldman BJ, Streeper RS, Farese RV, Yamamoto KR. Myostatin modulates adipogenesis to generate adipocytes with favorable metabolic effects. Proc Natl Acad Sci U S A 2006;103(42):15675–80.
[16] Sharma M, Kambadur R, Matthews KG, Somers WG, Devlin GP, Conaglen JV, et al. Myostatin, a transforming growth factor-beta superfamily member, is expressed in heart muscle and is upregulated in cardiomyocytes after infarct. J Cell Physiol 1999;180(1):1–9.
[17] Hirai S, Matsumoto H, Hino N, Kawachi H, Matsui T, Yano H. Myostatin inhibits differentiation of bovine preadipocyte. Domest Anim Endocrinol 2007;32(1):1–14.
[18] Karsenty G, Ferron M. The contribution of bone to whole-organism physiology. Nature 2012;481(7381):314–20.
[19] Springer J, Adams V, Anker SD. Myostatin: regulator of muscle wasting in heart failure and treatment target for cardiac cachexia. Circulation 2010;121(3):354–6.
[20] Hamrick MW. Increased bone mineral density in the femora of GDF8 knockout mice. Anat Rec A: Discov Mol Cell Evol Biol 2003;272(1):388–91.
[21] Hamrick MW, McPherron AC, Lovejoy CO. Bone mineral content and density in the humerus of adult myostatin-deficient mice. Calcif Tissue Int 2002;71(1):63–8.
[22] Hamrick MW, McPherron AC, Lovejoy CO, Hudson J, et al. Femoral morphology and cross-sectional geometry of adult myostatin-deficient mice. Bone 2000;27(3):343–9.
[23] Hamrick MW, Pennington C, Byron CD. Bone architecture and disc degeneration in he lumbar spine of mice lacking GDF-8 (myostatin). J Orthop Res 2003;21(6):1025–32.
[24] Nicholson EK, Stock SR, Hamrick MW, Ravosa MJ. Biomineralization and adaptive plasticity of the temporomandibular joint in myostatin knockout mice. Arch Oral Biol 2006;51(1):37–49.
[25] Cho T-J, Gerstenfeld LC, Einhorn TA. Differential temporal expression of members of the transforming growth factor beta superfamily during murine fracture healing. J Bone Miner Res 2002;17(3):513–20.
[26] Kellum E, Starr H, Arounleut P, Immel D, Fulzele S, Wenger K, et al. Myostatin (GDF-8) deficiency increases fracture callus size, Sox-5 expression, and callus bone volume. Bone 2009;44(1):17–23.
[27] Amling M, Takeda S, Karsenty G. A neuro (endo)crine regulation of bone remodeling. Bioessays 2000;22(11):970–5.
[28] Souza TA, Guo Y, Sava P, Zhang J, Hill JJ, et al. Proteomic identification and functional validation of activins and bone morphogenetic protein 11 as candidate novel muscle mass regulators. Mol Endocrinol 2008;22(12):2689–702.
[29] de Caestecker M. The transforming growth factor-beta superfamily of receptors. Cytokine Growth Factor Rev 2004;15(1):1–11.
[30] Rebbapragada A, Benchabane H, Wrana JL, Celeste AJ, Attisano L. Myostatin signals through a transforming growth factor beta-like signaling pathway to block adipogenesis. Mol Cell Biol 2003;23(20):7230–42.
[31] Pearsall RS, Canalis E, Cornwall-Brady M, Underwood KW, Haigis B, Ucran J, et al. A soluble activin type IIA receptor induces bone formation and improves skeletal integrity. Proc Natl Acad Sci U S A 2008;105(19):7082–7.
[32] Lee SJ, Reed LA, Davies MV, Girgenrath S, Goad ME, Tomkinson KN, et al. Regulation of muscle growth by multiple ligands signaling through activin type II receptors. Proc Natl Acad Sci U S A 2005;102(50):18117–22.
[33] Shuto T, Sarkar G, Bronk JT, Matsui N, Bolander ME. Osteoblasts express types I and II activin receptors during early intramembranous and endochondral bone formation. J Bone Miner Res 1997;12(3):403–11.
[34] Hamrick MW, Shi X, Zhang W, Pennington C, Thakore H, Haque M, et al. Loss of myostatin (GDF8) function increases osteogenic differentiation of bone marrow-derived mesenchymal stem cells but the osteogenic effect is ablated with unloading. Bone 2007;40(6):1544–53.
[35] Chen G, Deng C, Li YP. TGF-beta and BMP signaling in osteoblast differentiation and bone formation. Int J Biol Sci 2012;8(2):272–88.
[36] Karsenty G. Central control of bone formation. Ann Endocrinol (Paris) 2002;63(2 Pt 1):145–53.
[37] Daluiski A, Engstrand T, Bahamonde ME, Gamer LW, Agius E, Stevenson SL, et al. Bone morphogenetic protein-3 is a negative regulator of bone density. Nat Genet 2001;27(1):84–8.
[38] Gamer LW, Cox K, Carlo JM, Rosen V. Overexpression of BMP3 in the developing skeleton alters endochondral bone formation resulting in spontaneous rib fractures. Dev Dyn 2009;238(9):2374–81.
[39] Hill JJ, Davies MV, Pearsall AA, Wang JH, Hewick RM, Wolfman NM, et al. The myostatin propeptide and the follistatin-related gene are inhibitory binding proteins of myostatin in normal serum. J Biol Chem 2002;277(43):40735–41.

[40] Bogdanovich S, Krag TO, Barton ER, Morris LD, Whittemore LA, Ahima RS, et al. Functional improvement of dystrophic muscle by myostatin blockade. Nature 2002;420(6914):418–21.
[41] Glatt V, Canalis E, Stadmeyer L, Bouxsein ML. Age-related changes in trabecular architecture differ in female and male C57BL/6J mice. J Bone Miner Res 2007;22(8):1197–207.
[42] Seeherman HJ, Bouxsein M, Kim H, Li R, Li XJ, Aiolova M, et al. Recombinant human bone morphogenetic protein-2 delivered in an injectable calcium phosphate paste accelerates osteotomy-site healing in a nonhuman primate model. J Bone Joint Surg Am 2004;86-A(9):1961–72.
[43] Allen DL, Banstra ER, Harrison BC, Thorng S, Stodieck LS, Kostenuik PJ, et al. Effects of spaceflight on murine skeletal muscle gene expression. J Appl Physiol 2009;106(2):582–95.
[44] Lalani R, Bhasin S, Byhower F, Tarnuzzer R, Grant M, Shen R, et al. Myostatin and insulin-like growth factor-I and -II expression in the muscle of rats exposed to the microgravity environment of the NeuroLab space shuttle flight. J Endocrinol 2000;167(3):417–28.
[45] McMahon CD, Popovic L, Oldman JM, Jeanplong F, Smith HK, Kambadur R, et al. Myostatin-deficient mice lose more skeletal muscle mass than wild-type controls during hindlimb suspension. Am J Physiol Endocrinol Metab 2003;285(1):E82–7.
[46] Kawada S, Tachi C, Ishii N. Content and localization of myostatin in mouse skeletal muscles during aging, mechanical unloading and reloading. J Muscle Res Cell Motil 2001;22(8):627–33.
[47] Nguyen J, Tang SY, Nguyen D, Alliston T, et al. Load regulates bone formation and sclerostin expression through a TGFbeta-dependent mechanism. PLoS One 2013;8(1):e53813.
[48] Wolfman NM, McPherron AC, Pappano WN, Davies MV, Song K, Tomkinson KN, et al. Activation of latent myostatin by the BMP-1/tolloid family of metalloproteinases. Proc Natl Acad Sci U S A 2003;100(26):15842–6.
[49] Townson SA, Martinez-Hackert E, Greppi C, Lowden P, Sako D, Liu J, et al. Specificity and structure of a high affinity activin receptor-like kinase 1 (ALK1) signaling complex. J Biol Chem 2012;287(33):27313–25.
[50] Sako D, Grinberg AV, Liu J, Davies MV, Castonguay R, Maniatis S, et al. Characterization of the ligand binding functionality of the extracellular domain of activin receptor type IIb. J Biol Chem 2010;285(27):21037–48.
[51] Fajardo RJ, Manoharan RK, Pearsall RS, Davies MV, Marvell T, Monnell TE, et al. Treatment with a soluble receptor for activin improves bone mass and structure in the axial and appendicular skeleton of female cynomolgus macaques (*Macaca fascicularis*). Bone 2010;46(1):64–71.
[52] Lotinun S, Pearsall RS, Davies MV, Marvell TH, Monnell TE, Ucran J, et al. A soluble activin receptor Type IIA fusion protein (ACE-011) increases bone mass via a dual anabolic-antiresorptive effect in Cynomolgus monkeys. Bone 2010;46(4):1082–8.
[53] Ogawa Y, Schmidt DK, Nathan RM, Armstrong RM, Miller KL, Sawamura SJ, et al. Bovine bone activin enhances bone morphogenetic protein-induced ectopic bone formation. J Biol Chem 1992;267(20):14233–7.
[54] Fuller K, Bayley KE, Chambers TJ. Activin A is an essential cofactor for osteoclast induction. Biochem Biophys Res Commun 2000;268(1):2–7.
[55] Sakai R, Eto Y, Ohtsuka M, Hirafuji M, Shinoda H. Activin enhances osteoclast-like cell formation in vitro. Biochem Biophys Res Commun 1993;195(1):39–46.
[56] Sakai R, Miwa K, Eto Y. Local administration of activin promotes fracture healing in the rat fibula fracture model. Bone 1999;25(2):191–6.
[57] Sakai R, Fujita S, Horie T, Ohyama T, Miwa K, Maki T, et al. Activin increases bone mass and mechanical strength of lumbar vertebrae in aged ovariectomized rats. Bone 2000;27(1):91–6.
[58] Perrien DS, Akel NS, Edwards PK, Carver AA, Bendre MS, Swain FL, et al. Inhibin A is an endocrine stimulator of bone mass and strength. Endocrinology 2007;148(4):1654–65.
[59] Esbrit P, Alcaraz MJ. Current perspectives on parathyroid hormone (PTH) and PTH-related protein (PTHrP) as bone anabolic therapies. Biochem Pharmacol 2013;85(10):1417–23.
[60] Chiu CS, Peekhaus N, Weber H, Adamski S, Murray EM, Zhang HZ, et al. Increased muscle force production and bone mineral density in ActRIIB-Fc-treated mature rodents. J Gerontol A Biol Sci Med Sci 2013;68(10):1181–92.
[61] Papapoulos SE. Targeting sclerostin as potential treatment of osteoporosis. Ann Rheum Dis 2011;70(Suppl. 1):i119–22.
[62] Rhee Y, Lee EY, Lezcano V, Ronda AC, Condon KW, Allen MR, et al. Resorption controls bone anabolism driven by parathyroid hormone (PTH) receptor signaling in osteocytes. J Biol Chem 2013;288(41):29809–20.
[63] Badhi D, Jang G, Stouch B, Fang L, Posvar E. Single-dose, placebo-controlled, randomized study of AMG 785, a sclerostin monoclonal antibody. J Bone Miner Res 2011;26(1):19–26.
[64] Fernandez-Garcia D, Munoz-Torres M, Mezquita-Raya P, de la Higuera M, Alonso G, et al. Effects of raloxifene therapy on circulating osteoprotegerin and RANK ligand levels in post-menopausal osteoporosis. J Endocrinol Invest 2008;31(5):416–21.
[65] Cummings SR, San Martin J, McClung MR, Siris ES, Eastell R, Reid IR, et al. Denosumab for prevention of fractures in postmenopausal women with osteoporosis. N Engl J Med 2009;361(8):756–65.
[66] Tsai JN, Uihlein AV, Lee H, Kumbhani R, Siwila-Sackman E, McKay EA, et al. Teriparatide and denosumab, alone or combined, in women with postmenopausal osteoporosis: the DATA study randomised trial. Lancet 2013;382(9886):50–6.
[67] Bonnick S, De Villiers T, Odio A, Palacious S, Chapurlat R, Dasilva C, et al. Effects of odanacatib on BMD and safety in the treatment of osteoporosis in postmenopausal women previously treated with alendronate: a randomized placebo-controlled trial. J Clin Endocrinol Metab 2013(12):4727–35.
[68] Liu J, Xu K, Wen G, Guo H, Li S, Wu X, et al. Comparison of the effects of genistein and zoledronic acid on the bone loss in OPG-deficient mice. Bone 2008;42(5):950–9.